Nonlinear Control of Ball and Beam System

***Abstract*—We report the implementation of two controllers on the ball and beam system, the PID controller and the LQR controller with feedback linearization and Luenberger observer (FL+LQR). The two controllers are examined in both simulation and hardware experiments. The results show that the PID controller outperforms FL+LQR controller. The source code can be found at https://github.com/meganteng/Nonlinear-project-group-1.**

I. Introduction

The ball and beam system is a canonical benchmark for evaluating control strategies on unstable, nonlinear systems [1], [2]. Its dynamics present significant challenges, including inherent instability and nonlinearities dependent on the beam angle. This work addresses the control objective of stabilizing the ball and tracking reference trajectories using this platform.

We present the design, simulation, and hardware implementation of two distinct controllers: a Proportional-Integral-Derivative (PID) controller and a Linear Quadratic Regulator integrated with Input-Output Feedback Linearization (FL+LQR) [3]. Due to limited sensor availability (only ball position z and beam angle θ are measured), a Luenberger observer is designed to estimate the full state vector required for the FL+LQR approach.

The primary contribution of this paper is the comparative evaluation of these two controllers, assessing their tracking performance and control effort in both simulation and hardware experiments. The following sections detail the system modeling (Section II), the observer and controller design methodologies (Section III), simulation results (Section IV), hardware experiment results (Section V), and finally, conclusions drawn from the comparative analysis (Section VI).

II. System Modeling

This work addresses the control of the Quanser Ball and Beam system [4]. This setup consists of a metal ball rolling along a beam, which is pivoted at its center and tilted by a servo motor connected via a lever arm. The control input u is the voltage applied to the servo motor, which actuates the beam angle θ. The objective is to control the position z of the ball along the beam.

The system's dynamics are modeled using a state vector $x = [z, \dot{z}, \theta, \dot{\theta}]^\top$, which includes the ball position, ball velocity, beam angle, and beam angular velocity, respectively. The system can be modelled by the nonlinear state equations $\dot{x} = f(x, u)$ given by:

$$\dot{x} = f(x,u) = \begin{bmatrix} x_2 \\ \frac{5gr_{\text{arm}}}{7L}\sin(x_3) - \frac{5}{7}\left(\frac{L}{2} - x_1\right)\left(\frac{r_{\text{arm}}}{L}\right)^2 x_4^2 \cos^2(x_3) \\ x_4 \\ \frac{-x_4 + K_{\text{motor}}u}{\tau} \end{bmatrix}$$

where $x_1 = z, x_2 = \dot{z}, x_3 = \theta, x_4 = \dot{\theta}$. The physical parameters $g, r_{\text{arm}}, L, K_{\text{motor}}, \tau$ represent gravitational acceleration, servo arm length, beam length, motor gain, and motor time constant, respectively. Their specific values are listed in the Appendix (Tables IV and V).

The measured outputs for feedback are the ball position z and the beam angle θ. The output equation is $y = h(x) = Cx$, where the output matrix C is defined as:

$$C = \begin{bmatrix} 1 & 0 & 0 & 0 \\ 0 & 0 & 1 & 0 \end{bmatrix} \tag{1}$$

A. Linearized System Model

For linear controller design (LQR) and observer synthesis, the nonlinear model is linearized around the equilibrium point $x_0 = [0, 0, 0, 0]^\top$ and $u_0 = 0$. This yields the linear time-invariant (LTI) state-space representation $\dot{x} \approx Ax + Bu$, where the state matrix $A = \frac{\partial f}{\partial x}\Big|_{x_0,u_0}$ and input matrix $B = \frac{\partial f}{\partial u}\Big|_{x_0,u_0}$ are calculated as:

$$A = \begin{bmatrix} 0 & 1 & 0 & 0 \\ 0 & 0 & \frac{5gr_{\text{arm}}}{7L} & 0 \\ 0 & 0 & 0 & 1 \\ 0 & 0 & 0 & -\frac{1}{\tau} \end{bmatrix}, \tag{2}$$

$$B = \begin{bmatrix} 0 \\ 0 \\ 0 \\ \frac{K_{motor}}{\tau} \end{bmatrix} \tag{3}$$

The output matrix C (Eq. (1)) remains unchanged for the linearized system. The detailed derivation of the Jacobian matrices used for linearization can be found in the Appendix.

For digital implementation, a discrete-time model is required. Using a sampling time $dt = 0.01$ s, the continuous-time system (Eqs. (2), (3), (1)) is discretized using a zero-order hold method:

$$(A_d, B_d) = \texttt{c2d}(A, B, dt).$$

The discrete output matrix is simply $C_d = C$.

III. Observer and Controller Design

This section details the theoretical formulations of the observer and two control strategies implemented to stabilize and track a reference trajectory for the ball-and-beam system. Each control approach was selected to explore trade-offs between simplicity, robustness, and optimality under model nonlinearity.

A. Observer Design

Due to limited sensor access, only the ball position z and beam angle θ are directly measured. We construct a Luenberger observer to estimate the full state vector:

$$x = \begin{bmatrix} z & \dot{z} & \theta & \dot{\theta} \end{bmatrix}^\top, \quad y = \begin{bmatrix} z & \theta \end{bmatrix}^\top.$$

Continuous-Time Observer: We define the observer dynamics as:

$$\dot{\hat{x}} = A\hat{x} + Bu + L(y - C\hat{x}),$$

where $\hat{x}$ is the estimated state, u is the control input, and L is the observer gain. The matrices A, B, C correspond to the linearized state-space representation of the system. Observer poles are placed at locations four times faster than those of the closed-loop system:

$$\text{observer\_poles} = 4 \cdot \text{eig}(A - BK)$$
$$L = \texttt{place}(A^\top, C^\top, \text{observer\_poles})^\top.$$

Discrete-Time Observer: For digital control, we discretize the continuous-time model using zero-order hold:

$$(A_d, B_d) = \texttt{c2d}(A, B, dt),$$

and apply the discrete-time observer update:

$$\hat{x}[k+1] = A_d\hat{x}[k] + B_d u[k] + L_d(y[k] - C\hat{x}[k]),$$

where L_d is the discrete observer gain matrix. Poles are manually assigned within the unit circle to ensure rapid convergence and robustness:

$$L_d = \texttt{place}(A_d^\top, C^\top, \text{manual\_poles})^\top.$$

B. Control Method 1: PID Controller

The PID controller regulates the beam angle based on the error between the current and reference ball position. Define:

$$e(t) = z(t) - z_{\text{ref}}(t).$$

The controller output is the desired beam angle:

$$\theta_d(t) = -K_p e(t) - K_i \int_0^t e(\tau)d\tau - K_d \frac{d}{dt}e(t).$$

In practice, this is implemented via discretized updates:

$$\begin{aligned} \text{error} &= z - z_{\text{ref}}, \\ \text{integral\_error} &+= \text{error} \cdot dt, \\ \text{derivative\_error} &= \frac{\text{error} - \text{prev\_error}}{dt}, \\ \theta_d &= -K_p \cdot \text{error} - K_i \cdot \text{integral\_error} \\ &\quad - K_d \cdot \text{derivative\_error}. \end{aligned}$$

This angle is bounded by physical saturation:

$$\theta_d = \text{clip}(\theta_d, -\frac{\pi}{4}, \frac{\pi}{4}),$$

and converted to a servo voltage using:

$$V = k_{\text{servo}}(\theta_d - \theta).$$

The calculated servo voltage V is then saturated to adhere to actuator limits $[\pm V_{\max}]$ as a safety precaution.

C. Control Method 2: Full-State LQR with Feedback Linearization

This method combines optimal full-state feedback with input-output feedback linearization to compensate for system nonlinearities and achieve precise trajectory tracking.

LQR Design: Using the linearized model:

$$\dot{x} = Ax + Bu,$$

we solve the LQR problem:

$$J = \int_0^\infty \left(x^\top Q x + u^\top R u\right) dt,$$

with $Q = \text{diag}(100,\, 0.3,\, 0,\, 0)$, $R = 0.2$. The control law is:

$$v = -Kx + \ddot{z}_{\text{ref}}.$$

Feedback Linearization: The system has relative degree 3 with respect to output $y = z$, so we compute:

$$\dddot{z} = a\cos(\theta)\dot{\theta} + \mathcal{N}(x, \dot{x}),$$

where $a = \frac{5gr_g}{7L}$ and $\mathcal{N}(\cdot)$ contains all remaining nonlinear terms. Solving for the physical control input:

$$u = \frac{(v - \mathcal{N}) \cdot \tau}{a\cos(\theta)K}.$$

Beam Angle Inversion: To compute the target beam angle that corresponds to the desired acceleration:

$$\theta_d = \arcsin\left(\frac{7L}{5gr_g}\left[v + \frac{5}{7}\left(\frac{L}{2} - z\right)\left(\frac{r_g}{L}\right)^2 \dot{\theta}^2 \cos^2(\theta)\right]\right),$$

followed by saturation:

$$\theta_d = \text{clip}(\theta_d, -\frac{\pi}{4}, \frac{\pi}{4}), \quad V = k_{\text{servo}}(\theta_d - \theta).$$

The calculated servo voltage V is then saturated to adhere to actuator limits $[\pm V_{\max}]$ as a safety precaution.

Velocity Estimation: Since $\dot{z}$ and $\dot{\theta}$ are unmeasured, we estimate via finite differences:

$$\dot{z} \approx \frac{z(t) - z(t - \Delta t)}{\Delta t}, \quad \dot{\theta} \approx \frac{\theta(t) - \theta(t - \Delta t)}{\Delta t}.$$

IV. Simulation Results

The simulations are conducted with the same parameter combinations as the hardware experiments, which is Table II. Their control performance results are shown in Table I.

Figures 1, 2, 3 and 4 show the sine wave and square wave tracking trajectories and control inputs. Both PID and FL+LQR works well in sine wave tracking, but unsatisfactory on square wave tracking.

TABLE I
SIMULATION PERFORMANCE. AMPLITUDE OF SINE WAVE SET TO 0.08 M, AND OF SQUARE WAVE SET TO 0.04 M, AND PERIOD OF 10 SECONDS

Reference	Controller	Tracking Cost	Energy Cost	Total Score
Sine Wave	PID	0.13	0.00	**0.13**
	FL + LQR	1.75	1.88	3.64
Square Wave	PID	31.33	0.28	**41.61**
	FL + LQR	1.97	18.70	20.67

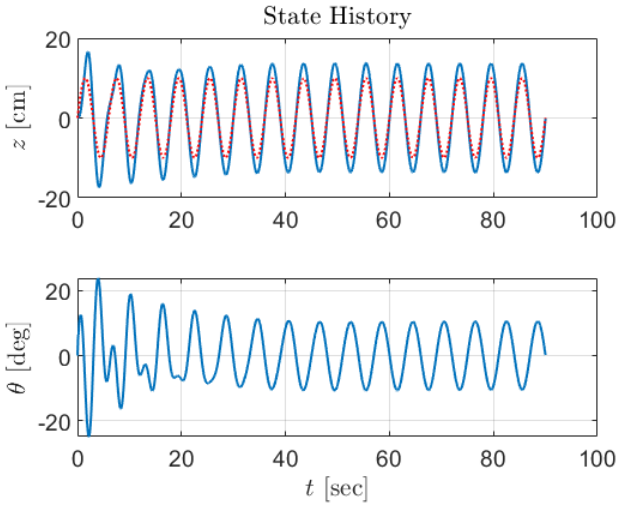

Fig. 1. Simulation results of PID closed-loop response when tracking a sine-wave reference. **Top:** Vertical displacement z in cm, where the solid **blue** line represents the system response and the dashed **orange** line represents the desired reference trajectory. **Bottom:** Angular displacement θ in degrees, showing the system's oscillatory response over time.

V. HARDWARE EXPERIMENT RESULTS

We implemented the PID and FL+LQR controllers on the hardware ball and beam system. The parameters are summarized in Table II and their performances are compared in Table III. During hardware experiments, we observed that the implemented FL+LQR controller, although performs very well in simulation, generated a highly oscillating control input. Although the tracking cost is reasonable, it has an extraordinary high energy cost. Adding low-pass filter can effectively smooth the control input, but the tracking cost significantly increased. On the other hand, the PID controller, despite its simple structure, generate much smoother control inputs, leading to a decreased energy cost. As such, in the ball and beam tracking system, we found that PID outperforms FL+LQR after careful tuning.

The tracking plots of the PID controller is shown in Fig. 5.

VI. CONCLUSION

We implemented two controllers on the ball and beam system, LQR with feedback linearization (FL+LQR) and PID controller. Luenberger observer is used in FL+LQR controller. The two controllers shows similar tracking results, but the control inputs of FL+LQR is highly oscillating, while PID

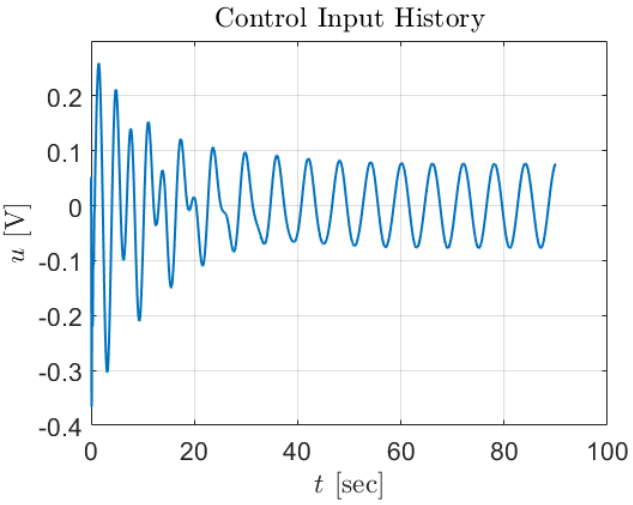

Fig. 2. Simulation result for PID closed-loop response, displaying control input voltage u over time during sine wave reference trajectory tracking.

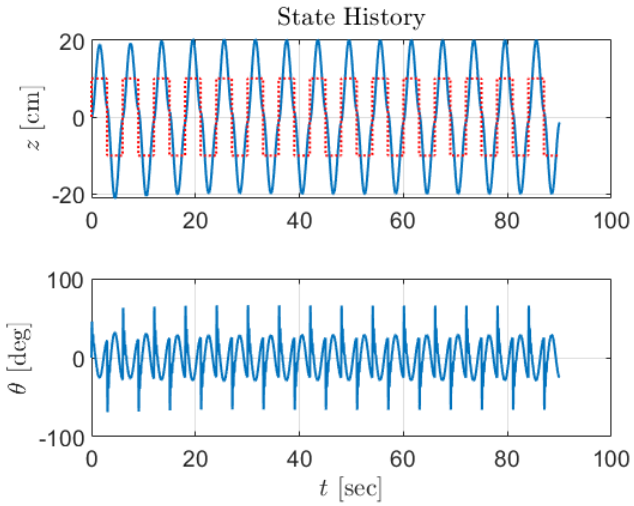

Fig. 3. Simulation results of PID closed-loop response when tracking a square-wave reference. **Top:** Vertical displacement z in cm, where the solid **blue** line represents the system response and the dashed **orange** line represents the desired reference trajectory. **Bottom:** Angular displacement θ in degrees, showing the system's oscillatory response over time.

control gives a much smoother control input. Therefore, PID shows better performance in ball and beam system.

We were very surprised by the huge sim-to-real gap of the ball-and-beam system. The FL+LQR controller yields satisfactory performance in simulation with a relatively low energy cost, but on hardware, its energy cost is significantly higher. Similarly for PID, the parameter combination that works well in simulation shows terrible performance on hardware. A significant amount of tuning was performed to make it work on hardware.

If we will do this lab again, we would only perform start directly from hardware experiments, since simulation is not at all reliable on predicting the controller's performance on hardware.

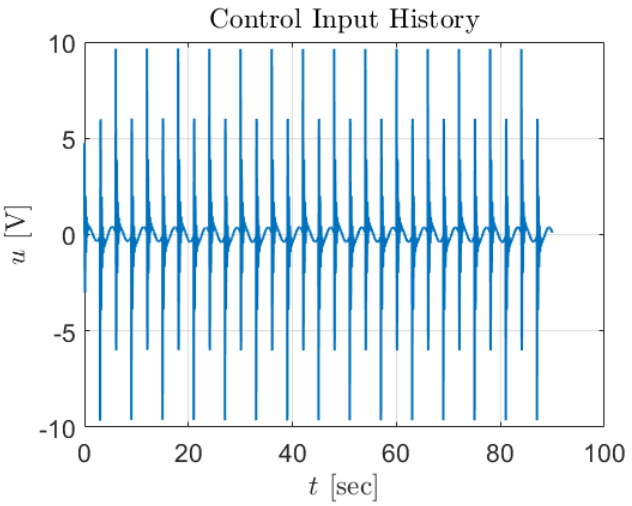

Fig. 4. Simulation result for PID closed-loop response, displaying control input voltage u over time during square wave reference trajectory tracking.

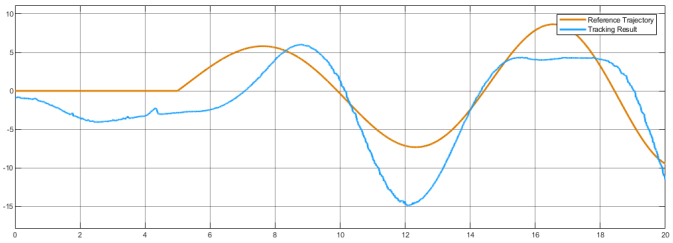

Fig. 5. Experimental hardware results of the PID controller tracking the evaluation trajectory. The **orange** curve indicates the reference position z_{ref} in cm, while the **blue** curve indicates the measured ball position z in cm.

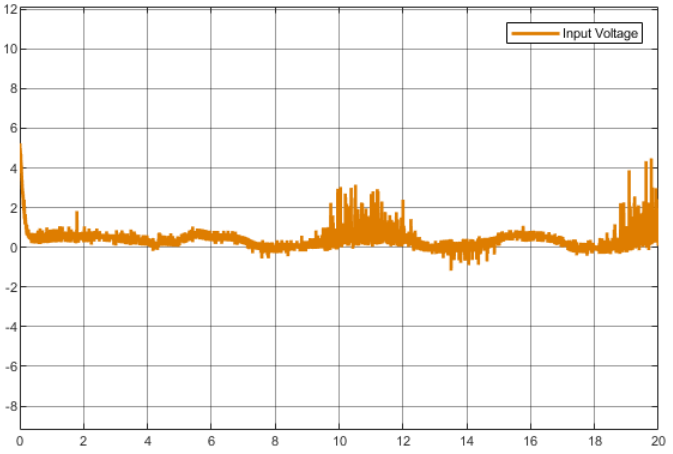

Fig. 6. Experimental hardware result for PID closed-loop response, displaying control input voltage u over time during reference tracking of the evaluation trajectory.

TABLE II
PID AND LQR+FL CONTROL PARAMETERSUSED IN HARDWARE EXPERIMENTS.

Controller	Q (diagonal)	R	P	I	D
PID	—	—	5	0	0.5
LQR + FL	$(298,\ 6.87,\ 0,\ 0)$	0.406	—	—	—

TABLE III
HARDWARE PERFORMANCE

Reference	**Controller**	**Tracking Cost**	**Energy Cost**	**Total Score**
Evaluation Trajectory	PID	2.51	1.91	**4.42**
	FL + LQR	3.32	255.38	258.70

REFERENCES

[1] J. Hauser, S. S. Sastry, and P. Kokotovic, "Nonlinear control via approximate input-output linearization: the ball and beam example," *IEEE Transactions on Automatic Control*, vol. 37, no. 3, pp. 392–398, March 1992.

[2] Y. Guo, D. J. Hill, and Z.-P. Jiang, "Global nonlinear control of the ball and beam system," in *Proceedings of 35th IEEE Conference on Decision and Control*, vol. 3, Kobe, Japan, 1996, pp. 2818–2823.

[3] R. Soni and Sathans, "Optimal control of a ball and beam system through lqr and lqg," in *2018 2nd International Conference on Inventive Systems and Control (ICISC)*, Coimbatore, India, 2018, pp. 179–184.

[4] Q. Inc., "Ball and beam module – control systems and dynamics," https://www.quanser.com/products/ball-and-beam/, 2025, accessed: 2025-05-02.

APPENDIX

The appendix provides the parameters and implementation details necessary to replicate our experiments of the the ball and beam system.

A. Ball and Beam Physical Parameters

Table IV lists all physical parameters of the ball and beam system used in our experiments.

TABLE IV
BALL AND BEAM PHYSICAL PARAMETERS

Parameter	Symbol	Value
Gravitational acceleration	g	9.81 m/s^2
Beam length	L	0.4255 m (16.75 in)
Servo arm length	r_{arm}	0.0254 m (1 in)
Ball radius	r_b	0.0127 m (0.5 in)
Ball mass	m_b	0.064 kg
Ball moment of inertia	J_b	$\frac{2}{5} m_b r_b^2$ kg·m^2
Beam angle limits	$\theta_{\min}, \theta_{\max}$	$\pm 45^\circ$ ($\pm \frac{\pi}{3.22}$ rad)
Ball position limits	$z_{\min}, z_{\max}$	± 0.25 m
Ball position sensor calibration gain	K_{BS}	$-L/10$ m/V

B. Servo Motor Parameters

Table V presents the parameters of the servo motor used in the experimental hardware.

TABLE V
SERVO MOTOR PARAMETERS

Parameter	Symbol	Value
Motor armature resistance	R_m	2.6 Ω
Motor torque constant	k_t	0.00767 N·m/A
Motor back-EMF constant	k_m	0.00767 V·s/rad
Internal gear ratio	K_{gi}	14
Gearbox efficiency	η_g	0.90
Motor efficiency	η_m	0.69
Motor time constant	τ	0.025 s
Motor gain	K_{motor}	1.5 rad/s/V
Servo gain	k_{servo}	10 V/rad
Maximum output voltage	V_{max}	24 V

C. Jacobian Matrix Derivation

Nonlinear state dynamics:

$$\dot{x} = f(x,u) = \begin{bmatrix} f_1 \\ f_2 \\ f_3 \\ f_4 \end{bmatrix} = \begin{bmatrix} x_2 \\ \frac{5gr}{7L}\sin(x_3) - \frac{5}{7}\left(\frac{L}{2} - x_1\right)\left(\frac{r}{L}\right)^2 x_4^2 \cos^2(x_3) \\ x_4 \\ -\frac{x_4}{\tau} + \frac{K\,u}{\tau} \end{bmatrix}$$

A-matrix:

$$A = \frac{\partial f}{\partial x} = \begin{bmatrix} 0 & 1 & 0 & 0 \\ \frac{5}{7}\left(\frac{r}{L}\right)^2 x_4^2 \cos^2(x_3) & 0 & \frac{5gr}{7L}\cos(x_3) + \frac{10}{7}\left(\frac{L}{2} - x_1\right)\left(\frac{r}{L}\right)^2 x_4^2 \sin(x_3)\cos(x_3) & -\frac{10}{7}\left(\frac{L}{2} - x_1\right)\left(\frac{r}{L}\right)^2 x_4 \cos^2(x_3) \\ 0 & 0 & 0 & 1 \\ 0 & 0 & 0 & -\frac{1}{\tau} \end{bmatrix}$$

B-matrix:

$$B = \frac{\partial f}{\partial u} = \begin{bmatrix} 0 \\ 0 \\ 0 \\ \frac{K}{\tau} \end{bmatrix}.$$

Linearization at the equilibrium: Equilibrium at $x_0 = [0,0,0,0]^\top,\ u_0 = 0$.

Using $\sin 0 = 0$, $\cos 0 = 1$ and $x_4 = 0$, one obtains

$$A\,\big|_{x_0,u_0} = \begin{bmatrix} 0 & 1 & 0 & 0 \\ 0 & 0 & \frac{5gr}{7L} & 0 \\ 0 & 0 & 0 & 1 \\ 0 & 0 & 0 & -\frac{1}{\tau} \end{bmatrix}, \quad B\,\big|_{x_0,u_0} = \begin{bmatrix} 0 \\ 0 \\ 0 \\ \frac{K}{\tau} \end{bmatrix}.$$

The output matrices remain

$$C = \begin{bmatrix} 1 & 0 & 0 & 0 \\ 0 & 0 & 1 & 0 \end{bmatrix}$$

D. Performance Evaluation Criteria

The controller performance was evaluated using a weighted sum of tracking error and control energy:

- Tracking cost: Mean squared error between actual and reference ball position
- Energy cost: Mean squared control voltage
- Total score: Sum of tracking cost and energy cost